INTERNATIONAL JOURNAL OF HYDROGEN ENERGY XXX (2015) 1–11

Available online at www.sciencedirect.com

ScienceDirect

journal homepage: www.elsevier.com/locate/he

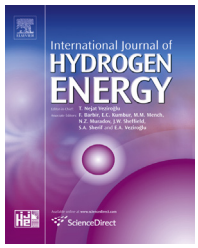

Advanced diagnosis based on temperature and current density distributions in a single PEMFC

Ali Mohammadi [a,b,*], *Abdesslem Djerdir* [a,b], *Nadia Yousfi Steiner* [b,c], *Davood Khaburi* [d]

[a] *Research Institute on Transportation, Energy and Society, Belfort Cedex, France*
[b] *FCLAB (FR CNRS 3539), 90010 Belfort Cedex, France*
[c] *Lab of Excellence ACTION CNRS/FEMTO-ST (UMR CNRS 6174) Energy Dpt, University of Franche-Comté, France*
[d] *Iran University of Science & Technology (IUST), 1684613114 Tehran, Iran*

ARTICLE INFO

Article history:
Received 28 January 2015
Received in revised form
24 April 2015
Accepted 29 April 2015
Available online xxx

Keywords:
Artificial Neural Network
Fault isolation
Temperature distribution
Voltage distribution
3D fault sensitive modeling
Proton exchange membrane fuel cells

ABSTRACT

The present study focuses on developing a reliable fault identification and localisation tool for Proton Exchange Membrane Fuel Cell (PEMFC). This diagnosis tool relies on 2 steps: first, a 3D model for a single PEMFC, that allows estimating local parameters (temperature, current and voltage distributions within the single cell). An experimental set-up allows reliable monitoring of different parameters used by the model to estimate the current density distributions over the 3D space zones of the cell. Furthermore, this 3D fault-sensitive model allows to simulate faults linked to poor water management (drying out and flooding) with 2 severity levels ("flooding", "drying", "high flooding" and "high drying").

Then, the second step consists of developing a two-layer feed-forward ANN that has been with an adapted database to localize each fault within the different segments of the single cell. The results show good recognition and localization rate for the considered fault, which allows to conclude that this approach is very promising for fault localization, which is one of the key points regarding diagnosis.

Introduction

PEMFCs are highly complex electrochemical systems based on electrocatalytic reactions: Hydrogen oxidation at the anode side and oxygen reduction at the cathode side. The operation of such systems involves several physical phenomena at different scales. Therefore, the degradation mechanisms are often complex, involving different parameters and phenomenon. For instance, improper water management could lead to Fuel Cell (FC) flooding or membrane drying out [1]. PEMFC could also face other faults like catalyst degradation, starvation and contamination [2–8]. These faults cause performance loss and could reduce drastically the FC lifetime.

Several parameters are involved in the operation of the FC and could affect its performance. Among these parameters, temperature appears to be one of the most performance-impacting, since it directly involves the reduction of voltage

* *Corresponding author*. IRTES, Rue Ernst THIERY MIEG, Bât B, Belfort Cedex 90010, France. Tel.: +33 384583629; fax: +33 384583636.
E-mail addresses: ali.mohammadi@utbm.fr (A. Mohammadi), abdesslem.djerdir@utbm.fr (A. Djerdir), nadia.steiner@univ-fcomte.fr (N. Yousfi Steiner), khaburi@iust.ac.ir (D. Khaburi).
http://dx.doi.org/10.1016/j.ijhydene.2015.04.157

Nomenclature

Roman symbols

E_r	the reverse voltage including the effect of gas pressures and temperature (V)
F	Faraday constant (96485 C Mol^{-1})
i	current density (A cm^{-2})
i_{lim}	limiting current density (A cm^{-2})
i_o	exchange current density (A cm^{-2})
T	temperature (K)
R	gas constant (8.314 J $Mol^{-1}K^{-1}$)
E	fuel cell stacks voltage (V)

Subscripts and superscripts

α	electron transfer coefficient, 0.5 for the Hydrogen fuel cell anode (with two electrons involved) and $\alpha = 0.1$ to 0.5 for the cathode
V_{act}	activation polarization (V)
V_{con}	concentration polarization (V)
V_{ohm}	Ohmic polarization (V)
V_C	voltage of the double layer effect (V)
PH_2	partial pressure of Hydrogen (Pa)
PO_2	partial pressure of oxygen (Pa)
R_{ohm}	equivalent membrane resistance (Ωcm^2)

through increasing the activation losses, or improving the conductivity of materials through increasing the diffusion coefficient. This was confirmed by Yan et *al* who studied and demonstrated the high impact of operating temperature on the current density value [9,10]. This is one of the reasons why, today the temperature and current density mappings are presented as the most advanced diagnostics methods for FCs [9–11].

Diagnosis of FC systems is a key topic that has been widely investigated in the last decades [12–18]. Due to the complexity of degradation mechanisms, many developments regarding FC diagnosis are however still needed.

In general, fault diagnosis could be classified into two main approaches: model-based and non-model based diagnosis approaches (Fig. 1).

Model-based methods rely on a valid model of the fuel cell, whose output is compared to the value measured on the actual operating fuel cell, which leads to the generation of residuals (see Fig. 1a). These latters are analyzed in order to achieve a decision on the FC's State of Health (SoH). Several kinds of models could be used for this approach; they could be either white-box (analytical models, with a complete description of the phenomena occurring in terms of mathematical equations), black-box (statically data) or a combination of the two, also called grey-box models [19–22]. Non-model based approaches, on the other hand, do not need any model of the system and use techniques from statistics, artificial intelligence or pattern recognition to achieve the diagnosis [23] (see Fig. 1b).

Artificial Neural Network (ANN) is one of the Artificial Intelligence approaches that has been widely and successfully applied to both control and diagnosis of the PEMFCs. It presents the advantage of being well adapted to non-linear systems modeling, either for regression or classification

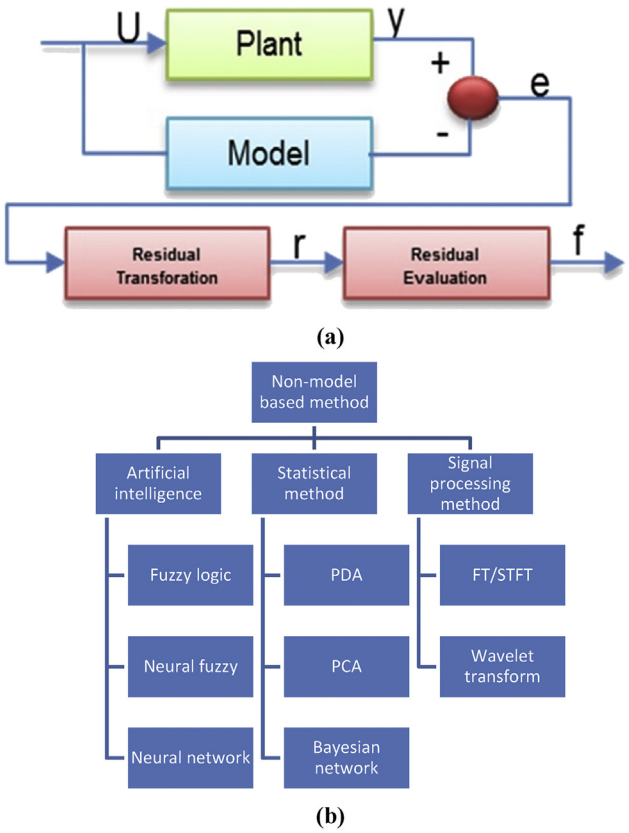

Fig. 1 – Model-based fault diagnosis diagram. [21],[23].

problems. Damour et al. [24] developed an ANN model of PEMFC in order to control oxygen excess ration in real time: the obtained results highlighted very low computational time compared to other nonlinear model-based controllers. On the other hand, Kumbur et al. used an ANN for the design of the gas diffusion layer of a fuel cell [25] while Justesen et al. [26] used the same model combined with fuzzy logic (Adaptive Neuro-Fuzzy Inference System (ANFIS)) in order to model gas composition in an FC. This kind of models has also been successfully applied in the work of Silva Sanchez et al. [27] to diagnostics/prognostics purposes in PEMFCs.

All these references used the ANN as a black-box model, without taking into account the 3D space geometry of the FC. Moreover, only very few articles in the literature took into account the strong relationship existing between the operating parameters with the related behaviors of the FC and the fault occurrence. Even if these models were able to give an accurate decision on the occurring faults, no fault localization was possible since the FCs have been considered as a whole, and no local parameters have been monitored or estimated.

In a more advanced diagnosis of the single fuel cell, information about the local parameter (for instance, through a special cell design that allows monitoring the current density or temperature distributions) is required. Besides the localisation, none of the above mentioned papers allowed to study the severity of the faults, as well.

This paper proposes a 2 steps diagnosis approach: first a 3D model has been developed in order to obtain a mapping of temperature, voltage and current density in the 3D space of

Please cite this article in press as: Mohammadi A, et al., Advanced diagnosis based on temperature and current density distributions in a single PEMFC, International Journal of Hydrogen Energy (2015), http://dx.doi.org/10.1016/j.ijhydene.2015.04.157

the fuel cell and then an ANN-based model is used to classify and localize different SoHs. The studied faults (flooding and drying out with 2 severity levels for each) are simulated by introducing abnormal variations of the critical operating conditions for water management, namely temperature, relative humidity of the gases, pressure of the inlet gases and current density. The faults are also simulated in certain zones of the 3D model so that to teach the ANN model the localization of the faults: therefore, the developed ANN algorithm aims to localize and evaluate the severity of flooding and drying out faults.

This paper will be organized as follows: first, the used diagnosis PEMFC method and the role of temperature distribution are discussed in part 1. Then, the proposed 3D fault sensitive model in terms of its general structure and physical parameters are explained in part 2. The Newton–Raphson Method (NRM) for the calculation of the current density used for the model calibration is presented part 3. The experimental setup dedicated to calibrate the proposed model, as well as the obtained results, are presented in part 4. Finally, before giving the concluding remarks of this work, it is shown how the artificial neural network algorithm was developed for faults localisation.

The 3D fault sensitive model

In order to obtain localized fault diagnosis of a PEMFC cell, the knowledge of the local behavior of different parameters is needed (Fig. 2). A Therefore, 3D fault-sensitive model is proposed in this study in order to obtain the temperature and current density distributions: the basic idea behind this model is the segmentation of the a cell into different elementary cells. 9 nodes in total have been defined and the cell divided into 9 segments in the two space directions (x and y axes), as shown in Fig. 3a and b. Each node is represented by one elementary electric equivalent circuit (circuit branch presented in Fig. 3c), that allows modeling the local behavior.

Fig. 3c represents the elementary electric equivalent circuit used in this study. This simple electric circuit is commonly used in the literature to model the main physical behavior of a PEM fuel cell, using the electric-mechanics/fluidics analogy. Thanks to the different electric elements in the circuit, this simple model is able to take into account dynamic phenomena occurring both at the anode and cathode such as activation polarization (R_{act}), ohmic polarization (R_{ohm}), double layer capacitance (C) and mass transport effects (R_{con}) present in a PEM fuel cell.

In this simplified model, the membrane is the main contributor to the ohmic losses, which means, the value of R_{ohm} reflects mainly the hydration of the membrane (ionic transfer), all fluidic contributions (gas transport within the flow fields and GDL are represented by the value of R_{con}), while the double layer capacitance will represent the dynamics of charge transfer at the interface membrane-electrode.

Besides, all nodes are connected to different resistances in the x and y axes in order to take into account the voltage drops between different nodes. The resistances between nodes are named according to their location. Setting the transverse coordinates for each node according to the node's number, that is to say, (X_1, Y_1) for the node N_1, (X_2, Y_2) for the node N_2 and so on, the resistor R_{12} is set between the nodes N_1 and N_2, the resistor R_{23} is set to N_2 and N_3,…etc. That means the index of each resistor contains the two numbers of the departure and the arrival node respectively: index 12 means departure node is N_1 arrival node is N_2. Thus, the total cell behavior in terms of current and voltage is obtained by the total contributions of the 9 electric circuits. The Newton–Raphson method is used to calibrate this model, as will be explained in the next section.

Fig. 3a and b show a side view of the complete electrical model, including the different resistances and capacitances. The magnitude of the voltage drop, called "voltage variance", is associated to the changes in fuel cell model parameters including open-circuit voltage, losses on the anode side (R_{act}, R_{Con}) losses in the cathode (R_{act}, R_{Con}) double layer capacitance (C) in anode and cathode and membrane losses (R_{ohm}) [28–30].

Current density distribution computation

The Newton-Raphshon method is used to find the current density distribution from voltage and temperature measurements. Based on the calculation of the current density, the 3D

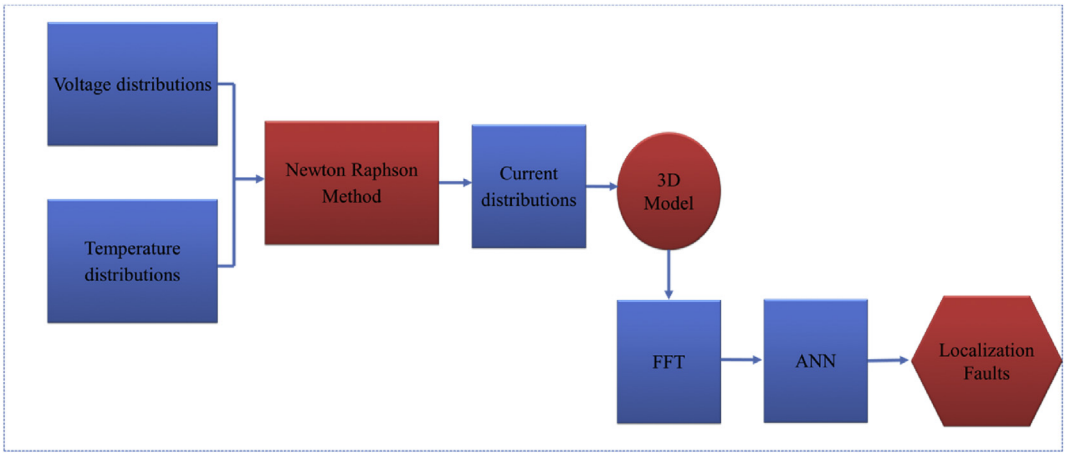

Fig. 2 – Faults detection process in PEMFC.

Please cite this article in press as: Mohammadi A, et al., Advanced diagnosis based on temperature and current density distributions in a single PEMFC, International Journal of Hydrogen Energy (2015), http://dx.doi.org/10.1016/j.ijhydene.2015.04.157

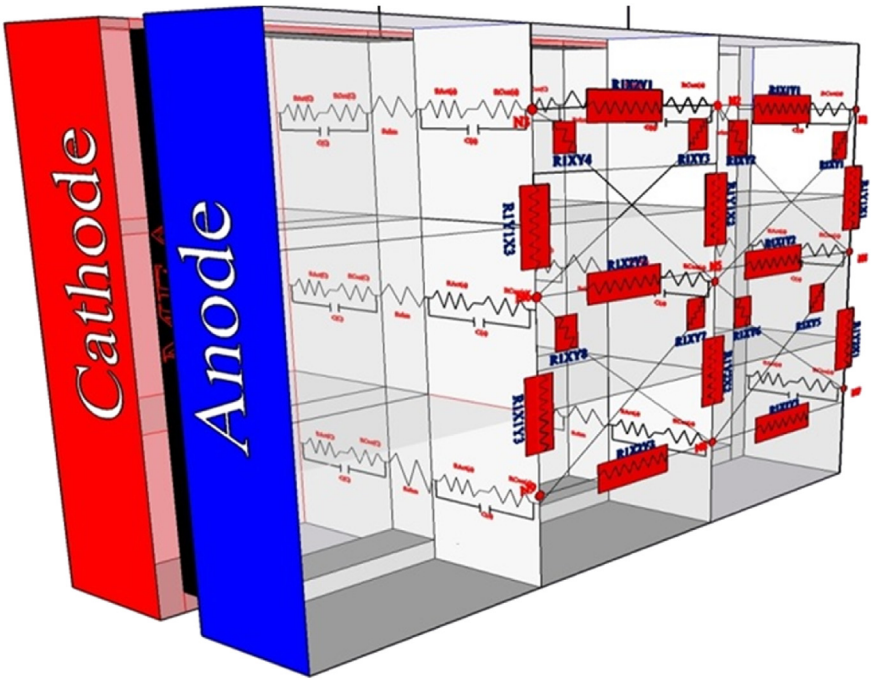

(a)

Fig. 3 – PEMFC based on the elementary cell in three dimensions (3D).

model can be calibrated by adding different resistances in the different space directions.

The Newton–Raphson method or Newton method is a powerful technique for solving equations numerically. In this work, the Newton–Raphson method is used to calculate the current density for each element, from the measured values of temperature and voltage. The Newton–Raphson problem sets of the two operations below [31]:

A) To assume the function $f = E - V$,where E is defined as the voltage calculation of the cell in each node [28–30]. This calculation is performed starting from the physical parameters of each elementary circuit evaluated analytically by using the measured temperature and voltage distributions. V is defined as the voltage measurements of each node (V).

$$E = E_r - V_{act} - V_{con} - V_{ohm} \tag{1}$$

$$E_r - 1.299 - 0.000845\ (T - 273.15) + 0.000431 \cdot T \cdot \ln\left(P_{H_2} \cdot P_{O_2}\right) \tag{2}$$

$$V_{act} = \frac{R \cdot T}{\alpha \cdot F} \ln\left[\frac{i}{i_0}\right] \tag{3}$$

$$V_{ohm} = i \cdot R_m \tag{4}$$

$$R_m = \frac{181.6\left[1 + 0.03i + 0.062\left(\frac{T}{303}\right)^2 \cdot i^{2.5}\right]}{e^{\left(4.18\left(\frac{T-303}{T}\right)\right)} \cdot [RH - 0.634 - 3i]}. \tag{5}$$

$$V_{con} = \frac{R \cdot T}{n \cdot F} \ln\left(\frac{I_{lim}}{I_{lim} - i}\right) \tag{6}$$

Notice that, based on the formulation above, many parameters such as temperature, pressure, charge transfer, exchange current density, Hydrogen crossover/external currents, resistance and limiting current can directly impact the performance of the fuel cell. Thus, Because of the difficulty in measuring data of humidity, pressure and other parameters in each node of the single cell, only variation temperature is considered in NRM.

B) find the current density distribution to reach the equality f(x) = 0,where, x vector is the distribution of the searching current density.

Given a function f defined over the real x, and its derivative f', we start with a first guess x_0 for a root of the function f. Provided the function that satisfies all the assumptions made in the derivation of the formula, a better approximation x_1 is expressed as:

$$x_1 = x_0 - \frac{f(x_0)}{f'(x_0)} \tag{7}$$

The process is repeated:

$$x_{n+1} = x_n - \frac{f(x_n)}{f'(x_n)}\ , \tag{8}$$

then the algorithm of Newton–Raphson method contains the seven main steps given below:

Step 1) Measurement of temperature and voltage in each node.
Step 2) Calculation of voltage of each node based on formulation above.
Step 3) Numerical Evaluation.

Please cite this article in press as: Mohammadi A, et al., Advanced diagnosis based on temperature and current density distributions in a single PEMFC, International Journal of Hydrogen Energy (2015), http://dx.doi.org/10.1016/j.ijhydene.2015.04.157

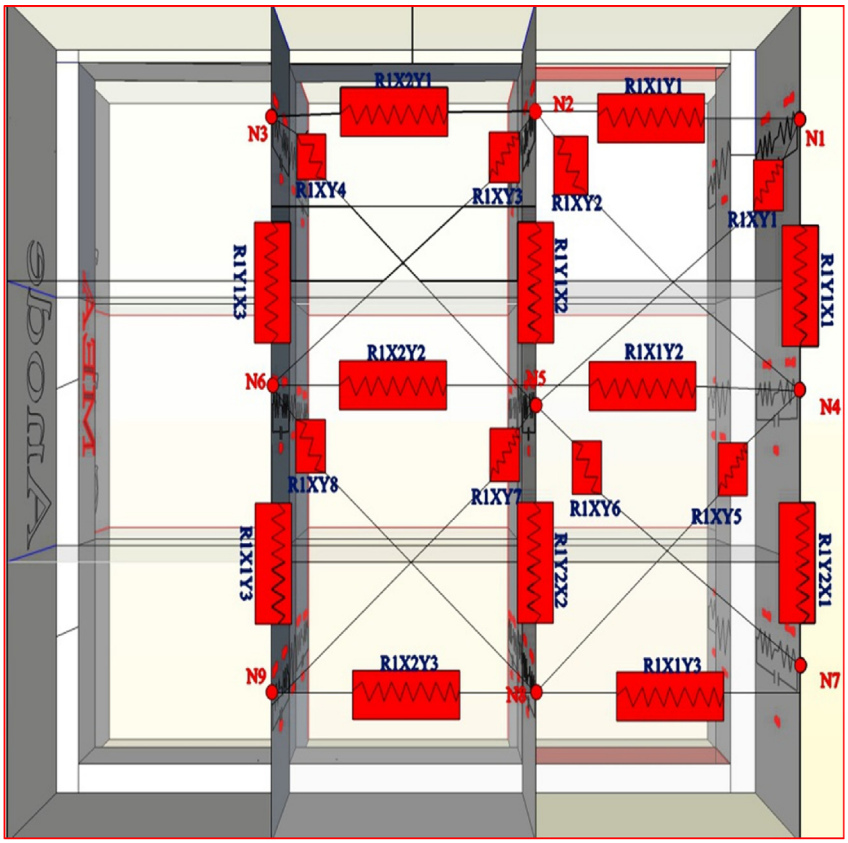

Fig. 3 – (*continued*).

Step 4) Utilization of an initial guess of the current density to estimate the new value of the current density, as in Equation (6).

Step 5) Calculation of the absolute, relative approximate error as:

$$|\varepsilon| = \left|\frac{x_{i+1} - x_i}{x_{i+1}}\right| \times 100 \quad (9)$$

Step 6) Comparison of the absolute, relative, approximate error with the pre-specified relative error tolerance.

- ➢ If > Relative error tolerance, to upgrade the initial guess of the current density and go to "step 4".
- ➢ If < Relative error tolerance, then go to "step 7" - stop the algorithm.

Step 7) Stop the Algorithm.

Temperature and voltage distributions are needed to start the algorithm of Newton–Raphson.

Experimental setup and model calibration

Experimental set-up

In order to measure the 12 voltages and 12 temperature values, a test bench for a single fuel cell has been carried out, 12 thermocouples and 12 voltage sensors are installed in different positions so that to be as closer as possible to the 9 elementary cells (segments) representation (see Fig. 4).

These sensors perform the measurements of the voltage between the anode (reference voltage) and cathode sides of each single cell as shown in Fig. 5. These voltage sensors were glued directly using an acceptable adhesive to the bipolar plate layer and isolated from the current connector as shown in Fig. 5.

Several tests have been run with the following operating conditions:

1 Air stoichiometry of 3 and Hydrogen stoichiometry of 2.
2 Current load of 10 A.

Please cite this article in press as: Mohammadi A, et al., Advanced diagnosis based on temperature and current density distributions in a single PEMFC, International Journal of Hydrogen Energy (2015), http://dx.doi.org/10.1016/j.ijhydene.2015.04.157

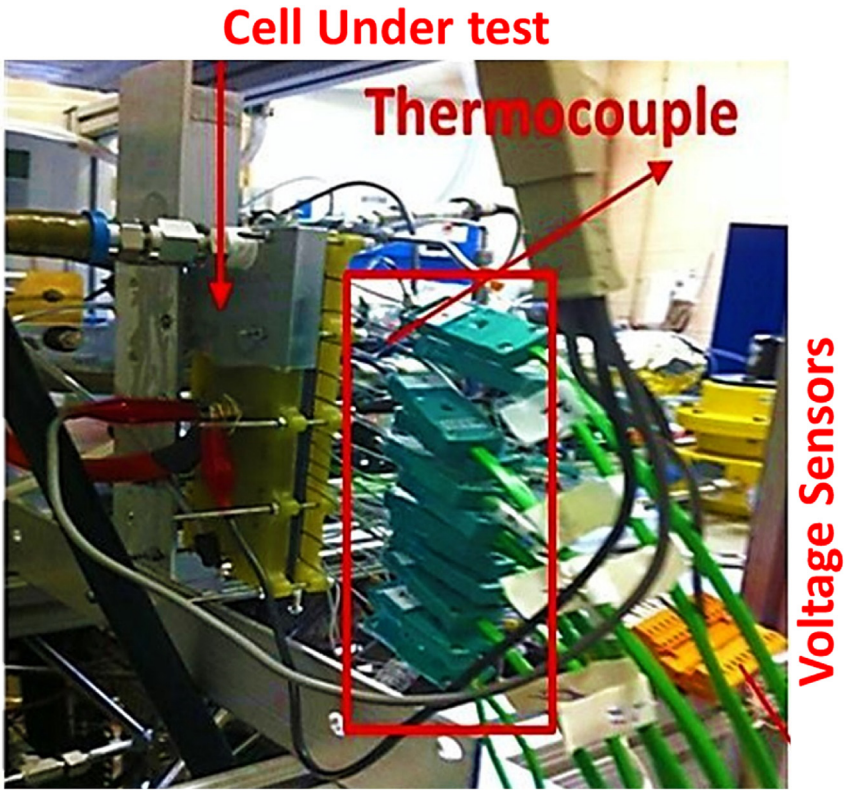

Fig. 4 – Set up measuring the voltage and thermocouple in PEMFC.

3 Humidified cathode (different relative humidities, RH%) and dry gas Hydrogen are used.

Model calibration

The temperature and voltage distributions that should be used to calculate the current distributions with the Newton–Raphson method are obtained experimentally. Table 1 indicates the measured temperatures and voltages while Table 2 gives the calculated current distribution.

In order to calculate impedances in different directions for the fuel cell, the calculation of the local current density has to be achieved at each node, based on the Newton–Raphson method (see Table 2). Table 3 reports the calculated resistances based on the current density.

To validate the obtained model, a simulation of the polarization curve has been performed (see Fig. 6). Comparing the results of the simulation to the experimental measurements, one can say that the model of FC is valid in the healthy state of health. This model will be used to simulate the faults.

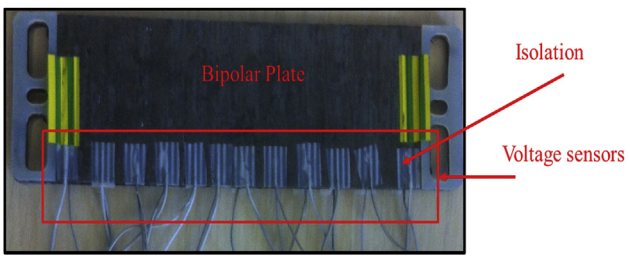

Fig. 5 – Sensors installation in single cell.

Flooding and drying faults characterization

In this section, the flooding and drying faults are characterized by using the developed 3D model. Both faults are consequences of a disequilibrium in water management; Flooding faults are simulated by setting the relative humidity to 100%,

Table 1 – Temperature and voltage distributions.

T(°C)	Left	Middle	Right
Inlet	25.65	29.09	29.53
Middle	33.5	31.12	31.41
Outlet	30.71	32.42	35.8
V(V)	Left	Middle	Right
Inlet	0.692	0.695	0.687
Middle	0.68	0.682	0.667
Outlet	0.685	0.674	0.652

Table 2 – Current distributions calculated by the Newton–Raphson method.

I(A)	Left	Middle	Right
Inlet	1.16	1.11	1.12
Middle	1.27	1.19	1.19
Outlet	1.35	1.24	1.17

Please cite this article in press as: Mohammadi A, et al., Advanced diagnosis based on temperature and current density distributions in a single PEMFC, International Journal of Hydrogen Energy (2015), http://dx.doi.org/10.1016/j.ijhydene.2015.04.157

Table 3 – Calculations of resistances in x, y axis.

Current load	Resistances in x, y axis					
10 (A)	R11[Ω]	$9.7\ e^{-4}$	R14[Ω]	$4.85\ e^{-4}$	R15[Ω]	$4.5\ e^{-4}$
	R23[Ω]	$1.89\ e^{-4}$	R25[Ω]	$5.1\ e^{-4}$	R24[Ω]	$1.452\ e^{-3}$
	R45[Ω]	$9.3\ e^{-4}$	R36[Ω]	$2.43\ e^{-3}$	R26[Ω]	$2.59\ e^{-3}$
	R56[Ω]	$2.08\ e^{-3}$	R47[Ω]	$1.27\ e^{-3}$	R35[Ω]	$3.2\ e^{-4}$
	R78[Ω]	$1.656\ e^{-3}$	R58[Ω]	$3.83\ e^{-3}$	R48[Ω]	$2.9\ e^{-3}$
	R89[Ω]	$3.83\ e^{-3}$	R69[Ω]	$2.06\ e^{-3}$	R57[Ω]	$2.19\ e^{-3}$
			R59[Ω]	$2.77\ e^{-5}$		
			R68[Ω]	$1.78\ e^{-3}$		

pressure to 2.2 bar and temperature adjusted between 40 and 55 °C. The drying out fault is simulated with a constant pressure value, a temperature ranging between 50 °C and 60 °C and a humidity rate ranging from 50% to 80%. "high flooding" corresponds to high humidity range from 100% to 120% (liquid water introduced), with a pressure value from 1 to 2.2 bar and a temperature value between 55 °C and 60 °C, while the "high drying out" SoH corresponds to a constant pressure value of 1 bar, a temperature of 62 °C and a humidity rate adjusted between 30% and 50%. Table 4 summarizes all these information.

Analytical calculations of current density based on the Newton–Raphson method under different faults are shown in Table 5 and Table 6. In these tables; all effects of the faults in each node are shown in grey rectangle boxes. It can be observed that the local current density has the highest values in the case where the FC faces a "high flooding" fault and decreases when it experiences "high drying" faults. Flooding faults cause the local current density to increase because the ohmic resistance decreases suddenly. However, drying out makes the local current density reduce, because the ohmic resistance increases.

Finally, all these information are collected into a database of different parameters corresponding to different type of faults ("flooding", "high flooding", "drying out", "high drying out") and different locations of the faults (9 locations in total corresponding to the 9 segments of the cell) has been generated and will be used to train the ANN.

Artificial Neural Network

ANN algorithm development and training

An Artificial Neural Network (ANN) is a combination of numerous neurons that are connected together via weighted connections. ANN are powerful tools for fault classification [32–34]. The ANN advantages consist in their ability to model complex non-linear relationships in a simple way.

In this work, a two-layer feed-forward ANN has been used in order to isolate different faults ("flooding", "drying out", "high flooding" and "high drying out") as illustrated in Fig. 7.

The information used by the ANN in this work comes from the voltage of each sub-cell and depends strongly on the operating conditions. A preprocessing of the voltage signal thanks to a Fast Fourier Transform (FFT) has been applied in order to extract the 7 first harmonic attributes that will be used as input to the ANN, for each of the 9 segments.

In fact, the frequency content of the voltage signal and in particular harmonics is usually rich information used for fault

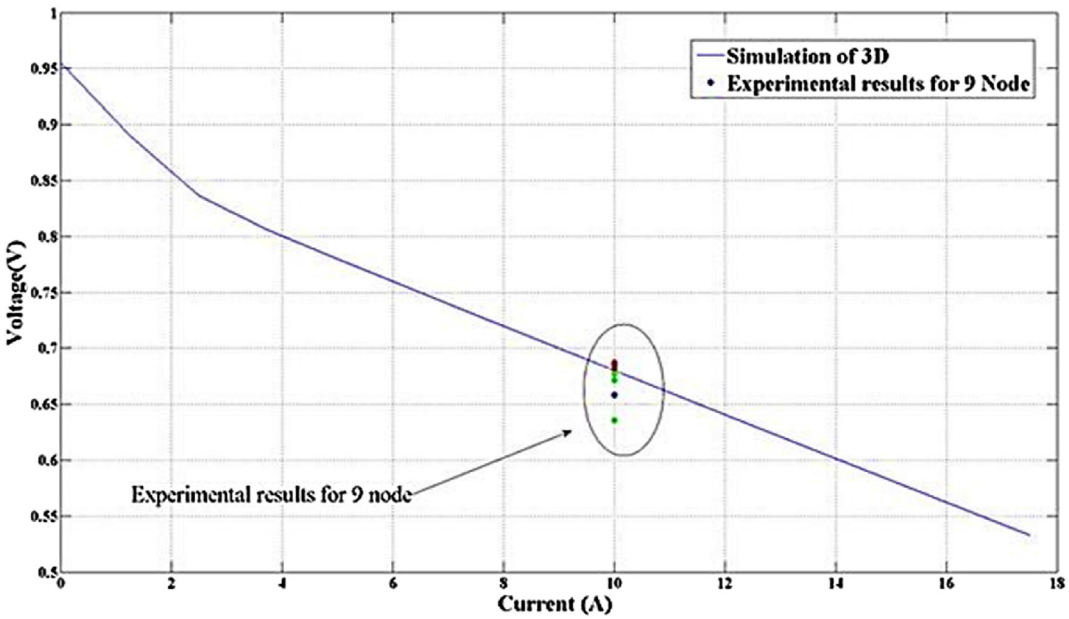

Fig. 6 – Validation simulation and experimental test for one cell.

Please cite this article in press as: Mohammadi A, et al., Advanced diagnosis based on temperature and current density distributions in a single PEMFC, International Journal of Hydrogen Energy (2015), http://dx.doi.org/10.1016/j.ijhydene.2015.04.157

Table 4 – Classification of flooding and drying.

Fuel cell mode	Temperature (°C)	Humidity (%)	Pressure (bar)
High drying	>62	30–50	Constant
Drying	50–60	50–80	Constant
High flooding	55–60	100–120	1–2.2
Flooding	40–55	100	2.2

diagnosis. In our work, we choose to use only the first 7 harmonics coming from the FFT and in order to prove that these attributes are fault sensitive, we calculate the corresponding Harmonic Distortion Rate (HDR) and observed its evolution in function of the mean values voltage variation (MVV), both in presence and absence of faults, as represented in Fig. 8. This figure shows that, in presence of faults, the harmonics values change compared to the normal operating conditions in all the cell regions (even if the amplitude of change is higher for the middle and low part of the cell). Therefore, the 7 first harmonics could be considered as a good indicator of fault occurrence, and will thus, be used as an input parameter of

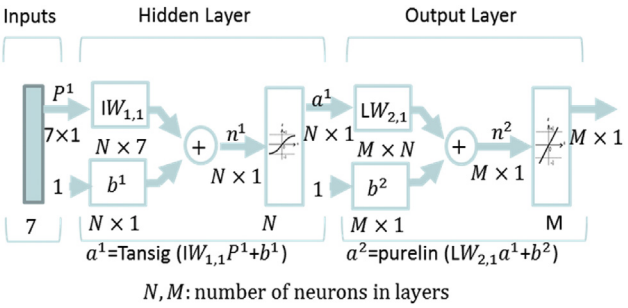

Fig. 7 – The architecture of feed-forward of artificial neural network.

the ANN model. For each fault, the ANN output corresponds to the location of the faults (1 choice out of 9).

The database reflecting the occurrence of each of the four faults: "flooding", "high flooding", "drying out", "high drying out" has been organized into input matrix X and target matrix

Table 5 – Local current density distribution in different nodes based on the "high flooding" and the "high drying" of 10 current profiles.

High drying									High flooding								
F3: T = 62 °C RH = 30%			F2: T = 62 °C RH = 30%			F1: T = 62 °C RH 30%			F3: T = 55 °C RH = 120%			F2: T = 55 °C RH = 120%			F1: T = 55 °C RH = 120%		
1.16	1.17	0.74	1.16	0.77	1.16	0.78	1.17	1.15	1.10	1.12	1.10	1.10	1.24	1.10	1.25	1.11	1.09
1.15	1.17	1.13	1.15	1.17	1.13	1.15	1.17	1.13	1.22	1.11	1.07	1.09	1.11	1.07	1.09	1.11	1.07
1.13	1.12	1.16	1.13	1.12	1.16	1.13	1.11	1.15	1.08	1.06	1.10	1.08	1.06	1.10	1.07	1.06	1.09
F6: T = 62 °C RH = 30%			F5: T = 62 °C RH = 30%			F4: T = 62 °C RH = 30%			F6: T = 55 °C RH = 120%			F5: T = 55 °C RH = 120%			F4: T = 55 °C RH = 120%		
1.16	1.17	1.158	1.16	1.18	1.16	1.16	1.17	1.15	1.10	1.12	1.10	1.10	1.12	1.10	1.10	1.12	1.10
1.14	1.17	0.762	1.15	0.77	1.13	0.76	1.17	1.13	1.09	1.11	1.20	1.09	1.23	1.07	1.09	1.23	1.07
1.13	1.11	1.158	1.13	1.12	1.16	1.13	1.11	1.15	1.08	1.06	1.10	1.08	1.06	1.10	1.08	1.06	1.10
F9: T = 62 °C RH = 30%			F8: T = 62 °C RH = 30%			F7: T = 62 °C RH = 30%			F9: T = 55 °C RH = 120%			F8: T = 55 °C RH = 120%			F7: T = 55 °C RH = 120%		
1.16	1.17	1.16	1.16	1.17	1.15	1.16	1.17	1.15	1.10	1.11	1.10	1.10	1.12	1.10	1.10	1.12	1.10
1.15	1.17	1.133	1.14	1.17	1.13	1.14	1.17	1.13	1.09	1.11	1.07	1.09	1.11	1.07	1.09	1.11	1.07
1.13	1.12	0.772	1.13	0.75	1.15	0.76	1.11	1.15	1.08	1.06	1.23	1.08	1.17	1.10	1.20	1.06	1.10

Table 6 – Local current density distribution in different nodes based on the "flooding" and the "drying" of 10 current profiles.

Flooding									Drying								
F3:T = 45 °C RH = 110%			F2:T = 45 °C RH = 110%			F1: T = 45 °C RH = 110%			F3: T = 55 °C RH = 50%			F2: T = 55 °C RH = 50%			F1: T = 55 °C RH = 50%		
1.11	1.12	1.17	1.11	1.18	1.11	1.19	1.12	1.10	1.15	1.16	0.86	1.15	0.86	1.15	0.87	1.16	1.14
1.1	1.12	1.08	1.10	1.12	1.08	1.09	1.12	1.08	1.14	1.16	1.12	1.14	1.16	1.12	1.13	1.16	1.12
1.08	1.07	1.10	1.08	1.07	1.11	1.08	1.06	1.10	1.12	1.10	1.14	1.12	1.11	1.15	1.12	1.10	1.14
F6:T = 45 °C RH = 110%			F5:T = 45 °C RH = 110%			F4:T = 45 °C RH = 110%			F6:T = 55 °C RH = 50%			F5:T = 55 °C RH = 50%			F4:T = 55 °C RH = 50%		
1.11	1.12	1.10	1.11	1.12	1.11	1.11	1.12	1.10	1.15	1.16	1.14	1.15	1.16	1.15	1.15	1.16	1.14
1.1	1.12	1.15	1.10	1.17	1.08	1.16	1.12	1.08	1.13	1.16	0.84	1.14	0.86	1.12	0.85	1.16	1.12
1.08	1.07	1.10	1.08	1.07	1.11	1.08	1.07	1.10	1.12	1.10	1.14	1.12	1.11	1.15	1.12	1.10	1.14
F9:T = 45 °C RH = 110%			F8:T = 45 °C RH = 110%			F7:T = 45 °C RH = 110%			F9: T = 55 °C RH = 50%			F8:T = 55 °C RH = 50%			F7:T = 55 °C RH = 50%		
1.11	1.12	1.10	1.11	1.12	1.11	1.11	1.12	1.11	1.15	1.16	1.14	1.15	1.16	1.14	1.15	1.16	1.14
1.1	1.12	1.08	1.10	1.12	1.08	1.10	1.12	1.08	1.14	1.16	1.12	1.13	1.16	1.12	1.13	1.16	1.12
1.08	1.07	1.17	1.08	1.12	1.11	1.14	1.07	1.11	1.12	1.10	0.85	1.12	0.83	1.14	0.84	1.10	1.14

Please cite this article in press as: Mohammadi A, et al., Advanced diagnosis based on temperature and current density distributions in a single PEMFC, International Journal of Hydrogen Energy (2015), http://dx.doi.org/10.1016/j.ijhydene.2015.04.157

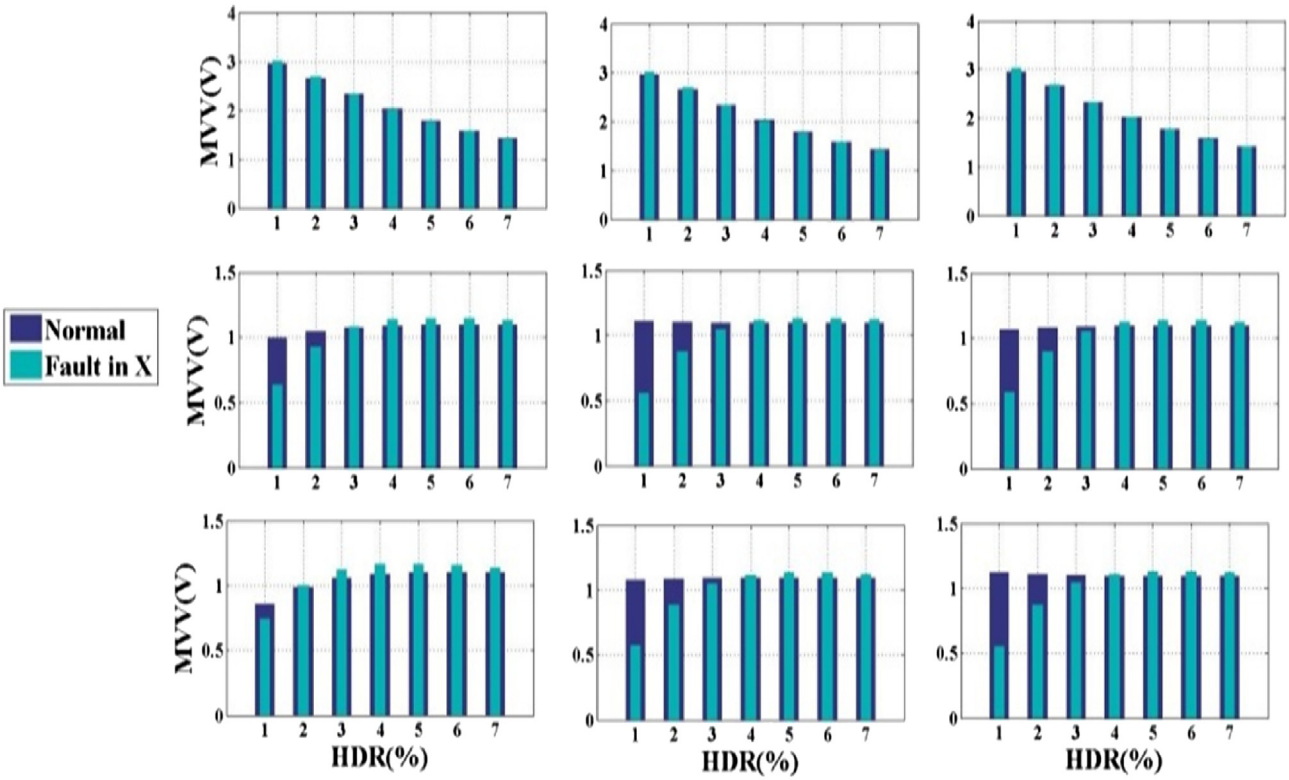

Fig. 8 – MVV and HDR variations according to resistance changes in x direction.

T. Each column of the input matrix will have 9 elements representing the 9 nodes, for each fault as shown in Fig. 7.

In total 2268 samples have been collected, 80% of which have been used for training, 10% for validation and 10% for testing the ANN.

For the "flooding" faulty mode for instance, a data set of 567 samples have been used. Fig. 9 shows the ANN training and the results of classification are presented in a "confusion matrix", shown in Fig. 9: this confusion matrix shows the percentage of correct and incorrect classification rates. Correct classifications are green squares on the diagonal. The results show a good ability to localize the fault, with a recognition rate of 97.5% in this case.

Conclusion

In this study, a 2 steps diagnosis approach for PEMFC has been presented. First, a 3D fault-sensitive model is built in order to estimate local parameters (temperature, current and voltage

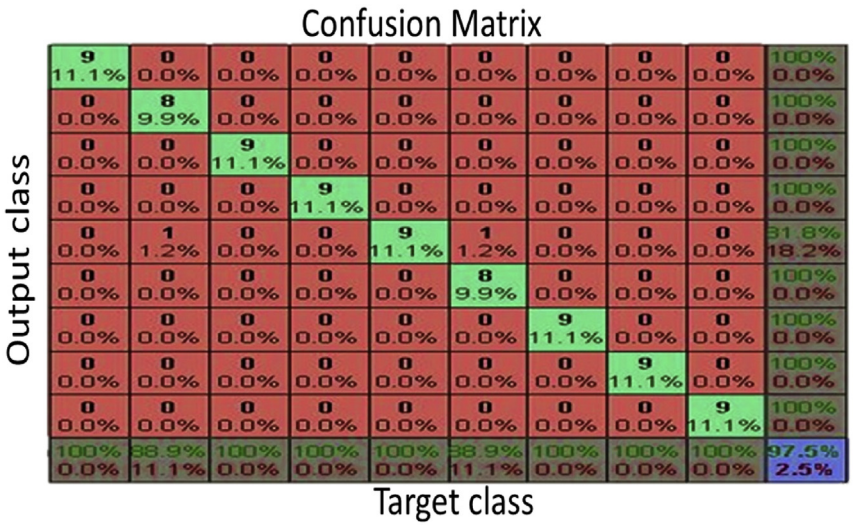

Fig. 9 – Fault isolation for flooding faults according to nine nodes during in one cell.

Please cite this article in press as: Mohammadi A, et al., Advanced diagnosis based on temperature and current density distributions in a single PEMFC, International Journal of Hydrogen Energy (2015), http://dx.doi.org/10.1016/j.ijhydene.2015.04.157

distribution within a single cell). It allows to simulate different faults (drying out and flooding) with 2 severity levels ("flooding", "drying", "high flooding" and "high drying").

Then, a two-layers feed-forward ANN has been developed. It is able to localize each fault in 9 considered segments within a single cell.

The results show good recognition and localization rate for the considered faults, which allows to conclude that this approach is very promising for fault localization, one of the key points regarding diagnosis.

The next step of this work is to carry on development based on this approach on a single cell, and generalize it to a stack. Further developments are related to the use of this algorithm for online detection, localization and classification of these faults and their severity on the real operating system.

Acknowledgments

This research work is carried out within the framework of MobyPost project funded under the Grant Agreement no. 256834 by the European Union's seventh Framework program (FP7/2007-2013) for the Fuel Cell and Hydrogen Joint Technology Undertaking (http://mobypostproject.eu/). Also, the authors acknowledge MES Company for providing the fuel cell and guidelines and the Labex ACTION (Contract ANR-11-LABX-0001-01) for its support.

REFERENCES

[1] Yousfi Steiner N, Hissel D, Moçotéguy P, Candusso D. Diagnosis of polymer electrolyte fuel cells failure modes (flooding & drying out) by neural networks modeling. Int J Hydrogen Energy Feb. 2011;36(4):3067–75.

[2] Yousfi-Steiner N, Moçotéguy P, Candusso D, Hissel D. A review on polymer electrolyte membrane fuel cell catalyst degradation and starvation issues: causes, consequences and diagnostic for mitigatio". J Power Sources Oct. 2009;194(1):130–45.

[3] Taniguchi A, Akita T, Yasuda K, Miyazaki Y. Analysis of degradation in PEMFC caused by cell reversal during air starvation. Int J Hydrogen Energy May 2008;33(9):2323–9.

[4] Giurgea S, Tirnovan R, Hissel D, Outbib R. An analysis of fluidic voltage statistical correlation for a diagnosis of PEM fuel cell flooding. Int J Hydrogen Energy Apr. 2013;38(11):4689–96.

[5] Li H, Tang Y, Wang Z, Shi Z, Wu S, Song D, et al. A review of water flooding issues in the proton exchange membrane fuel cell. J Power Sources Mars. 2008;178(1):103–17.

[6] Yousfi-Steiner N, Moçotéguy P, Candusso D, Hissel D, Hernandez A, Aslanides A. A review on PEM voltage degradation associated with water management: Impacts, influent factors and characterization. J Power Sources Aug. 2008;183(1):260–74.

[7] Hinaje M, Sadli I, Martin J-P, Thounthong P, Raël S, Davat B. Online humidification diagnosis of a PEMFC using a static DC–DC converter. Int J Hydrogen Energy Mars. 2009;34(6):2718–23.

[8] Wang HH, Li H, Yuan X-Z. Pem fuel cell diagnostic tool. CRC Press; 2011.

[9] Yan Q, Toghiani H, Causey H. Steady state and dynamic performance of proton exchange membrane fuel cells (PEMFCs) under various operating conditions and load changes. J Power Sources;161:492–502. http//dx.doi.org/10.1016/j.jpowsour.2006.03.077.

[10] Zhao D, Gao F, Massonnat P, Dou M, Miraoui A. Parameter sensitivity analysis and local temperature distribution effect for a PEMFC system. IEEE Trans Energy Convers:1–11. http//dx.doi.org/10.1109/TEC.2015.2404793.

[11] Barbir F. PEM fuel cells, second edition: theory and practice. 2 ed. Amsterdam ; Boston: Academic Press; 2012.

[12] de Lira S, Puig V, Quevedo J, Husar A. Robust LPV model-based sensor fault diagnosis using relative fault sensitivity signature and residual directions approaches in a PEM fuel cell. In: 2010 IEEE Vehicle Power and Propulsion Conference (VPPC); 2010. p. 1–7.

[13] Steiner NY, Hissel D, Moçotéguy P, Candusso D. Non-intrusive diagnosis of polymer electrolyte fuel cells by wavelet packet transform. Int J Hydrogen Energy Jan. 2011;36(1):740–6.

[14] de Beer C, Barendse P, Pillay P, Bullecks B, Rengaswamy R. Online fault diagnostics and impedance signature mapping of high temperature PEM fuel cells using rapid small signal injection. In: IECON 2013-39th Annual Conference of the IEEE Industrial Electronics Society; 2013. p. 1798–803.

[15] Zheng Z, Petrone R, Pera MC, Hissel D, Becherif M, Pianese C. Diagnosis of a commercial PEM fuel cell stack via incomplete spectra and fuzzy clustering. In: IECON 2013-39th Annual Conference of the IEEE Industrial Electronics Society; 2013. p. 1595–600.

[16] Hua J, Lu L, Ouyang M, Li J, Xu L. Proton exchange membrane fuel cell system diagnosis based on the signed directed graph method. J Power Sources Juill. 2011;196(14):5881–8.

[17] Wu J, Yuan XZ, Wang H, Blanco M, Martin JJ, Zhang J. Diagnostic tools in PEM fuel cell research: part I electrochemical techniques. Int J Hydrogen Energy Mars 2008;33(6):1735–46.

[18] Wu J, Zi Yuan X, Wang H, Blanco M, Martin JJ, Zhang J. Diagnostic tools in PEM fuel cell research: part II: physical/chemical methods. Int J Hydrogen Energy Mars 2008;33(6):1747–57.

[19] Isermann R. Model-based fault-detection and diagnosis – status and applications. Annu Rev Control 2005;29(1):71–85.

[20] Isermann R. Fault-diagnosis applications: model-based condition monitoring: actuators, drives, machinery, plants, sensors, and fault-tolerant systems. 2011 edition. New York: Springer; 2011.

[21] Petrone R, Zheng Z, Hissel D, Péra MC, Pianese C, Sorrentino M, et al. A review on model-based diagnosis methodologies for PEMFCs. Int J Hydrogen Energy Jun. 2013;38(17):7077–91.

[22] Venkatasubramanian V, Rengaswamy R, Yin K, Kavuri SN. A review of process fault detection and diagnosis: part I: quantitative model-based methods. Comput Chem Eng Mars 2003;27(3):293–311.

[23] Zheng Z, Petrone R, Péra MC, Hissel D, Becherif M, Pianese C, et al. A review on non-model based diagnosis methodologies for PEM fuel cell stacks and systems. Int J Hydrogen Energy Jul. 2013;38(21):8914–26.

[24] Damour C, Benne M, Lebreton C, Deseure J, Grondin-Perez B. Real-time implementation of a neural model-based self-tuning PID strategy for oxygen stoichiometry control in PEM fuel cell. Int J Hydrogen Energy;39:12819–25. http//dx.doi.org/10.1016/j.ijhydene.2014.06.039.

[25] Kumbur EC, Sharp KV, Mench MM. A design tool for predicting the capillary transport characteristics of fuel cell diffusion media using an artificial neural network. J Power Sources;176: 191–9. http//dx.doi.org/10.1016/j.jpowsour.2007.10.059.

Please cite this article in press as: Mohammadi A, et al., Advanced diagnosis based on temperature and current density distributions in a single PEMFC, International Journal of Hydrogen Energy (2015), http://dx.doi.org/10.1016/j.ijhydene.2015.04.157

[26] Justesen KK, Andreasen SJ, Shaker HR, Ehmsen MP, Andersen J. Gas composition modeling in a reformed methanol fuel cell system using adaptive neuro-fuzzy inference systems. Int J Hydrogen Energy;38:10577–84. http//dx.doi.org/10.1016/j.ijhydene.2013.06.013.
[27] Silva Sanchez R-E, Gouriveau R, Boulon L, Jemei S, Hissel D, Agbossou K, et al. Proton exchange membrane fuel cell degradation prediction based on adaptive neuro fuzzy inference systems. Int J Hydrogen Energy 2014;39:11128–44.
[28] Larminie J, Dicks A. Fuel cell systems explained. 2nd ed. Chichester, West Sussex: Wiley; 2003.
[29] Barbir F, Gorgun H, Wang X. Relationship between pressure drop and cell resistance as a diagnostic tool for PEM fuel cells. J Power Sources;141:96–101. http//dx.doi.org/10.1016/j.jpowsour.2004.08.055.2015.
[30] Springer TE, Zawodzinski TA, Gottesfeld S. Polymer electrolyte fuel cell model. J Electrochem Soc Aug. 1991;138(8):2334–42.
[31] Mohammadi A, Massonnat P, Djerdir A, Gao F, Krishnamurthy M, Bouquain D, et al. Fault analysis of the PEMFC by using 3D temperature fault sensitive model for automotive applications. Int J Energy Convers Sep 2014;2(5).
[32] "Neural Networks", Goodreads. Available sur: http://www.goodreads.com/work/best_book/380619-neural-networks-a-comprehensive-foundation. [Consulté le: 27-janv-2015].
[33] "Neural networks for modelling and control of dynamic systems", A practitioner's handbook.
[34] Steiner NY, Candusso D, Hissel D, Moçoteguy P. Model-based diagnosis for proton exchange membrane fuel cells. Math Comput Simul Oct. 2010;81(2):158–70.

Please cite this article in press as: Mohammadi A, et al., Advanced diagnosis based on temperature and current density distributions in a single PEMFC, International Journal of Hydrogen Energy (2015), http://dx.doi.org/10.1016/j.ijhydene.2015.04.157